

⁹Hamilton, H. H., Millman, D. R., and Greendyke, R. B., "Finite-Difference Solution for Laminar or Turbulent Boundary Layer Flow over Axisymmetric Bodies with Ideal Gas, CF₄ or Equilibrium Air Chemistry," NASA TP-3271, Dec. 1992.

¹⁰Fay, J. A., and Riddell, F. R., "Theory of Stagnation Point Heat Transfer in Dissociated Air," *Journal of the Aeronautical Sciences* Vol. 25, No. 2, 1958, pp. 73-85, 121.

T. C. Lin
Associate Editor

Wind Tunnel Simulation of Multibooster Separation Trajectories of a Launch Vehicle

H. Sundara Murthy* and G. K. Suryanarayana*
National Aerospace Laboratories, Bangalore, India
and

R. Lochan,† A. E. Sivaramakrishnan,† and S. Pandian†
Vikram Sarabhai Space Center, Trivandrum, India

Introduction

LAUNCH vehicles often incorporate multiple strap-on boosters as a design feature to achieve enhanced performance goals. Titan III, Delta 1914, Ariane, and Long March 2C are some of the launch vehicles featuring such boosters numbering from two to nine. When the burnt-out boosters are ejected from the advancing core, no collision should occur between the separated parts and the rest of the launch vehicle. During this process, the aerodynamic forces and moments acting on the separating bodies play a crucial role, especially when separation takes place at a high dynamic pressure. Various workers in the past (e.g., Refs. 1 and 2) have used conventional captive trajectory systems for determining the trajectory of a body separating from a launch vehicle. In these tests, however, a single body was separated from the parent body.

In the present paper, wind-tunnel investigations undertaken to study the separation characteristics of four strap-on boosters simultaneously separating from the core of a launch vehicle are described. The emphasis is on presenting the overall approach adopted for the investigations, and only some typical data are included. Similar work to determine the trajectories of two strap-on boosters simultaneously separating from a launch vehicle is reported in Ref. 3. The problem was handled in two phases. Initially, tests were conducted to generate extensive data by placing the boosters at a series of preselected locations and orientations in a region around the core. These tests, called grid tests, provided the necessary aerodynamic input for the design of the ejection mechanism.

The second phase of testing was undertaken after finalizing the design of the ejection mechanism and was essentially meant to ascertain its adequacy for safe separation of the boosters. A novel technique called the semicaptive-trajectory technique (SECTT) was adopted to accurately determine the trajectories of the four separating boosters for the most critical combination of parameters. SECTT is a semimanual version of the automatic captive-trajectory technique and is especially suited to handle multiple separating bodies in an intermittent wind tunnel with short-duration testing.

In the SECTT, the first wind-tunnel run is conducted with the boosters in their unseparated (frozen) position, and aerodynamic

loads on the separating boosters are measured. These data—along with other relevant parameters such as the mass-inertial properties of the booster, force-displacement history of the springs, etc.—are used to solve the Euler equations of motion for a short interval of time. This solution, which is carried out off line in a digital computer, gives the next position and orientation of each of the four boosters at the end of the integration period. The boosters are then manually moved to the new position and orientation, and the next test is carried out. Results from this test are utilized to obtain the subsequent position of the boosters. This step-by-step approach is continued till a description of the separation trajectories is obtained in the region of interest.

Description of the Model and the Experimental Set-Up

Figure 1 shows a sketch of the launch-vehicle model. It features six strap-on boosters and two secondary-injection thrust-vector control (SITVC) rockets clustered around a core vehicle. The boosters numbered 1 to 4 are equipped with two pairs of spring housings each and are designed to separate simultaneously at the design Mach number of 3.1. The other two boosters and the SITVC tanks remain fixed to the core vehicle.

A special test rig was built for the present study. The rig features four independent articulated support mechanisms for each of the boosters and a central sting for supporting the core vehicle. The articulated mechanism permits six-degree-of-freedom positioning of each of the four boosters. Figure 2 shows a photograph of the model mounted on the rig in the 1.2-m trisonic blowdown wind tunnel at the National Aerospace Laboratories (NAL).

Simulation of Dynamics and Related Software

A very general six-degree-of-freedom rigid-body model was derived for the separating boosters, whereas the core vehicle was assumed to be under ideal control. A set of 12 simultaneous first-order differential equations for each of the boosters was developed, and numerical integration performed using a modified Euler approach. The forces included for analysis are gravity, aerodynamic forces, thrust, tail-off thrust, and the spring forces of the ejection mechanism.

Two types of trajectories were determined using the SECTT. In the first case, the trajectory computations were performed using the measured aerodynamic coefficients and nominal values of other relevant parameters. The trajectory so obtained is termed the nominal trajectory. In the other case (called the perturbed trajectory), magnitudes of some of the measured and other important parameters were perturbed by their estimated uncertainty values in such a way that the resulting trajectory would be most unfavorable from the point of view of collision.

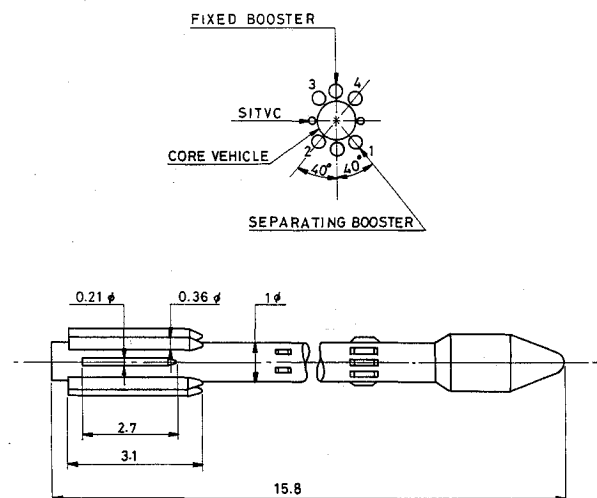


Fig. 1 Sketch of the model configuration.

Received Jan. 24, 1994; revision received Sept. 27, 1994; accepted for publication Oct. 5, 1994. Copyright © 1994 by the authors. Published by the American Institute of Aeronautics and Astronautics, Inc., with permission.

*Scientist.

†Engineer.

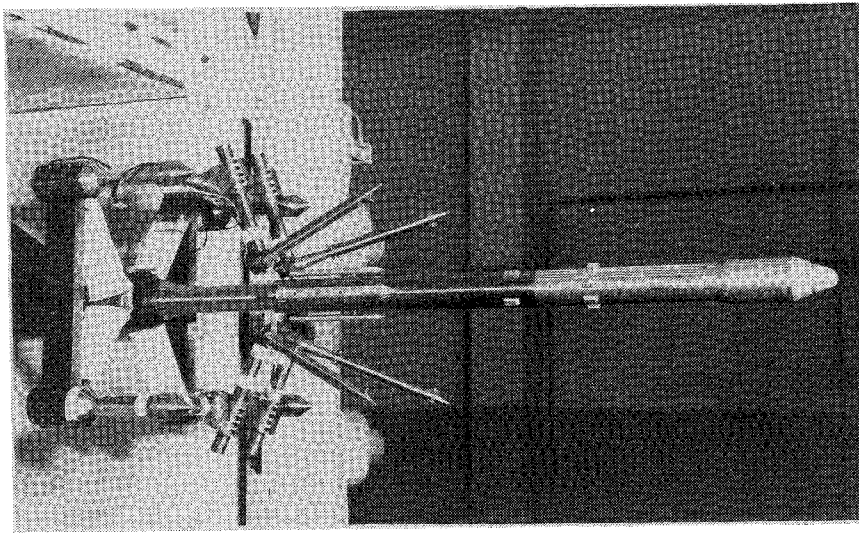


Fig. 2 Photograph of the model and the rig in the 1.2-m trisonic wind tunnel.

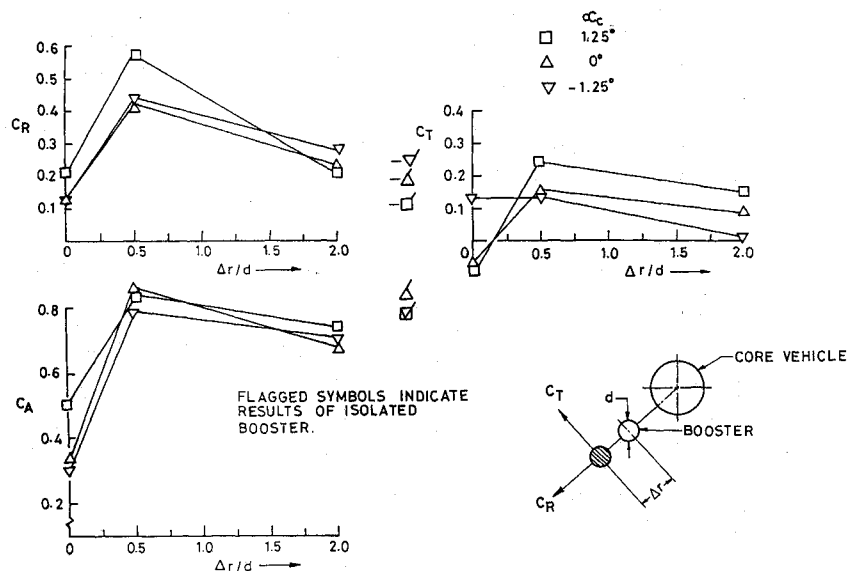


Fig. 3 Variation of aerodynamic forces on a separating booster with radial distance from the core vehicle.

Test Conditions

Tests were conducted in the NAL 1.2-m trisonic blowdown wind tunnel at a freestream Mach number of 3.1 and a test Reynolds number of $30.5 \times 10^6 \text{ m}^{-1}$. Force data for all the four boosters were obtained for a range of pitch angles between -3 and 3 deg. The data corresponding to the expected highest value of the pitch angle in flight viz., 1.5 deg, were utilized for the trajectory computations. Measurements were made using four 5-component (no rolling moment) internal strain-gauge balances, which were housed inside the four boosters.

Results and Discussions

Because of space restrictions, only some typical data from grid and trajectory tests are presented. The effects of increasing radial distance (Δr) on the aerodynamic forces on the separating booster are shown in Fig. 3 for three angles of attack (α_c) of the core vehicle. For better illustration of these effects, the coefficients obtained by resolving the measured normal and side forces along radial and tangential directions (C_R and C_T , respectively) are shown. The data obtained on the isolated booster are also included.

Aerodynamic forces on the boosters are strongly influenced by the flowfield of the other bodies located in its vicinity. For example, the forces on booster 1 will be influenced by the core, the fixed booster,

and the SITVC. In general, when the separating booster is not too close to the core, the nose shock waves from these bodies impinge on and are reflected from the surface of the separating booster, giving rise to increased pressure and consequently increased forces on the separating booster. The magnitude of forces due to such interference depends on the strength of the impinging shocks and the extent of surface area of the booster affected. The combined effect appears to become maximum at the intermediate position of the booster (the outward radial force was 2 to 3 times that on the isolated booster). As the distance between the booster and the core is further increased, the strength of the impinging shocks decreases, and so do the forces on the booster due to interference.

The forces on the booster located at its unseparated position ($\Delta r = 0$) are generally less than those at the isolated position. When the booster is close to the core, a part of the surface of the booster will be immersed in the boundary layer of the core and consequently a low-dynamic-pressure flow. When the booster is at its unseparated position, the gap between the surfaces of the booster and core was less than the sum of displacement thickness of the boundary layers on the two bodies. This is believed to be the main reason for the small aerodynamic forces at low values of Δr .

Typical results of separation trajectories obtained using the SECTT and schematic views of the four boosters are presented in

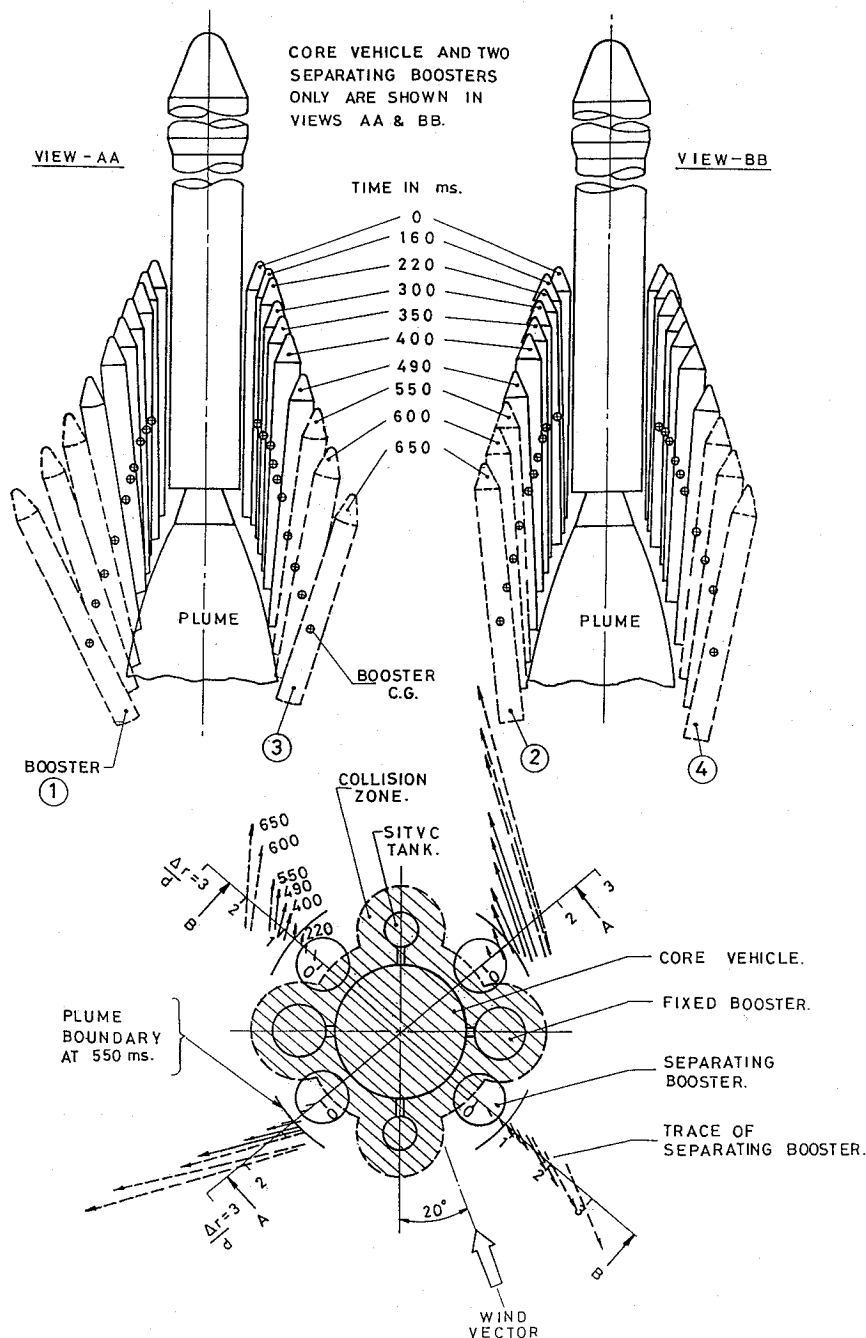


Fig. 4 Schematic of the separation trajectories.

Fig. 4. Traces of the centerline of each booster at different times reckoned from the initiation of separation process are also shown. The arrowhead of the trace represents the nose of the booster; the other end represents the center of the booster base. The region shown hatched in this view is termed the collision zone, since entry of any part of the trace of a booster into this region indicates a collision of the separating booster with one or more of the other parts of the vehicle. The positions of boosters shown in dashed lines were obtained using extrapolated aerodynamic data, since these positions were beyond the setting capability of the rig.

As seen from Fig. 4, gaps between the boosters and the core vehicle build up relatively slowly up to about 300 ms after initiation of separation (although the trajectory points were determined at an interval of 30 ms, the change in positions up to about 160 ms was too small to be shown in Fig. 4). Beyond 300 ms, the boosters move away from the core vehicle at a faster rate. Figure 4 also shows the estimated boundary of the plume from the core. It is seen that the traces of all the four boosters clear the collision zone, except that a

very small part of booster 1 penetrates the plume towards the end of the trajectory, which is not expected to cause any significant effect.

References

- Lanfranco, M. J., "Wind Tunnel Investigation of the Separation Maneuver of Equal-Size Bodies," *Journal of Spacecraft and Rockets*, Vol. 7, No. 11, 1970, pp. 1300-1305.
- Naftel, J. C., and Powell, R. W., "Analysis of the Staging Maneuver and Booster Glideback Guidance for a Two-Stage, Winged, Fully Reusable Launch Vehicle," NASA TP 3335, April 93.
- Sundara Murthy, H., Narayan, K. Y., Suryanarayana, G. K., Lochan, R., Nair, K. G. S., and Varambally, B. S., "Wind Tunnel Investigation of Strap-on Booster Separation Characteristics of a Launch Vehicle," *Journal of Aeronautical Society of India*, Vol. 38, No. 4, 1986, pp. 215-221.